Journal of
Plankton Research

plankt.oxfordjournals.org

J. Plankton Res. (2016) 38(4): 1077–1091. First published online January 23, 2016 doi:10.1093/plankt/fbv122

Contribution to the Themed Section: Scaling from individual plankton to marine ecosystems

Phytoplankton dynamics in the Southern California Bight indicate a complex mixture of transport and biology

STEPHAN BIALONSKI[1]*, DAVID A. CARON[2], JULIA SCHLOEN[3], ULRIKE FEUDEL[3], HOLGER KANTZ[1] AND STEFANIE D. MOORTHI[4]

[1]MAX PLANCK INSTITUTE FOR THE PHYSICS OF COMPLEX SYSTEMS, NÖTHNITZER STR. 38, 01187 DRESDEN, GERMANY, [2]DEPARTMENT OF BIOLOGICAL SCIENCES, UNIVERSITY OF SOUTHERN CALIFORNIA, 3616 TROUSDALE PARKWAY, AHF 301, LOS ANGELES, CA 90089-0371, USA, [3]INSTITUTE FOR CHEMISTRY AND BIOLOGY OF THE MARINE ENVIRONMENT (ICBM), UNIVERSITY OF OLDENBURG, CARL VON OSSIETZKY STR. 9-11, 26129 OLDENBURG, GERMANY AND [4]INSTITUTE FOR CHEMISTRY AND BIOLOGY OF THE MARINE ENVIRONMENT (ICBM), UNIVERSITY OF OLDENBURG, SCHLEUSENSTR. 1, 26382 WILHELMSHAVEN, GERMANY

*CORRESPONDING AUTHOR: bialonsk@pks.mpg.de

Received September 30, 2015; accepted December 11, 2015

Corresponding editor: Pia Moisander

The stimulation and dominance of potentially harmful phytoplankton taxa at a given locale and time are determined by local environmental conditions as well as by transport to or from neighboring regions. The present study investigated the occurrence of common harmful algal bloom (HAB) taxa within the Southern California Bight, using cross-correlation functions to determine potential dependencies between HAB taxa and environmental factors, and potential links to algal transport via local hydrography and currents. A simulation study, in which Lagrangian particles were released, was used to assess travel times due to advection by prevailing ocean currents in the bight. Our results indicate that transport of some taxa may be an important mechanism for the expansion of their distributions into other regions, which was supported by mean travel times derived from our simulation study and other literature on ocean currents in the Southern California Bight. In other cases, however, phytoplankton dynamics were rather linked to local environmental conditions, including coastal upwelling events. Overall, our study shows that complex current patterns in the Southern California Bight may contribute significantly to the formation and expansion of HABs in addition to local environmental factors determining the spatiotemporal dynamics of phytoplankton blooms.

KEYWORDS: phytoplankton; time-series; algal blooms; harmful algae; monitoring; SCCOOS; Southern California Bight; transport; coastal connectivity; Lagrangian particle tracking

available online at www.plankt.oxfordjournals.org

INTRODUCTION

Phytoplankton blooms are a common phenomenon of coastal ecosystems globally. These events have been well documented along the coast of the Southern California Bight, which typically exhibits significant spring blooms followed by several episodic blooms throughout the rest of the year (Nezlin and Li, 2003; Busse *et al.*, 2006; Schnetzer *et al.*, 2007; Anderson *et al.*, 2008; Shipe *et al.*, 2008; Kim *et al.*, 2009). Some of the bloom-forming algal species in this region may have harmful effects on local food webs (harmful algal blooms, HABs) and include potentially toxic species as well as non-toxic, high-biomass producers that can lead to hypoxia and anoxia and thus indiscriminant mortalities of marine life after reaching dense abundances (e.g. Kudela *et al.*, 2005; Heisler *et al.*, 2008). For instance, blooms of the toxic diatom *Pseudo-nitzschia* spp. have occurred frequently in coastal waters near Los Angeles throughout the last decade, and the San Pedro/Long Beach harbor region has been identified as a "hot spot" for outbreaks of marine animal mortality events attributed to the neurotoxin domoic acid (Schnetzer *et al.*, 2007, 2013). Additionally, massive red tides caused by the potentially toxic dinoflagellate *Lingulodinium polyedrum* sporadically occur along the coastline of Southern California (Allen, 1946; Holmes *et al.*, 1967; Gregorio and Pieper, 2000; Moorthi *et al.*, 2006; Shipe *et al.*, 2008; Omand *et al.*, 2011). These latter blooms have not yet been associated with marine animal or human illness in the area, even though the production of yessotoxin (a potential cardiotoxin) by this species has been confirmed (Howard *et al.*, 2008). Other toxin-producing or noxious phytoplankton genera that occur along the coast of Southern California include raphodiphyte and dinoflagellate species from the genera *Akashiwo*, *Alexandrium*, *Cochlodinium* and *Dinophysis* (Jessup *et al.*, 2009; Caron *et al.*, 2010; Garneau *et al.*, 2011; Howard *et al.*, 2012; Lewitus *et al.*, 2012).

Some of these HABs occur sporadically, whereas others appear on a regular annual basis, although their magnitude, the exact timing of their onset, their specific location and geographical extent within the bight, their composition (i.e. which species dominates) as well as their duration and termination vary significantly from year to year. Although this variability is believed to relate to a variety of physical, chemical and biological conditions (Pettersson and Pozdnyakov, 2013), it has proven difficult to accurately predict when and where blooms of particular species will occur. Coastal upwelling, specific hydrodynamics and land-based inputs of nutrients (major effluent discharges, river discharge and land runoff) have all been implicated as possible causes for HABs caused by *Pseudo-nitzschia* (Trainer *et al.*, 2000; Parsons *et al.*, 2002; Kudela *et al.*, 2005; Howard *et al.*, 2007; Anderson *et al.*, 2008) and dinoflagellates (Omand *et al.*, 2012; Reifel *et al.*, 2013).

The documentation of such bloom events and a comprehensive understanding of potential environmental conditions leading to them require long-term data sets of microalgal abundances and environmental parameters (Kim *et al.*, 2009; Glibert *et al.*, 2010; Frolov *et al.*, 2012). The Southern California Coastal Ocean Observing System (SCCOOS) HAB monitoring program was initiated in 2008 and is carried out by researchers from the California Polytechnic University, University of California Santa Barbara, University of California Los Angeles, University of Southern California and the Scripps Institution of Oceanography, University of California San Diego. This program entails weekly sampling from six different pier locations along the coast of Southern California (at the Cal Poly, Goleta, Stearns Wharf (SW), Santa Monica, Newport and Scripps piers). More recently, Santa Cruz Wharf and Monterey Wharf to the north of the Southern California Bight were added. Samples are analyzed for microalgal abundances, domoic acid in the particulate material in the water (produced by the toxic diatom *Pseudo-nitzschia* spp.) and nutrient concentrations, and basic chemical/physical parameters are provided by automated sensor packages maintained by SCCOOS (salinity) or hand-held instruments (temperature). Data from these sites are made publicly available through the SCCOOS website (http://www.sccoos.org/).

We employed a subset of the SCCOOS HAB data set obtained weekly at four different locations along the coast of the Southern California Bight to investigate the spatial patterns of algal bloom formation and propagation. Our goal was to differentiate the relative importance of growth of algal populations locally within the bight and dispersal between the sampling sites as factors explaining the timing of blooms and species composition of the algal community. Dispersal is largely non-random in the ocean. It is controlled by currents, which in turn are the result of an interplay among winds, tides and topography, and therefore usually directional.

Transport by prevailing ocean currents is a well-known mechanism for the propagation of HABs (Franks and Keafer, 2003), as shown, for instance, for *Alexandrium tamarense* (Franks and Anderson, 1992a, 1992b) and *Alexandrium fundyense* in the western Gulf of Maine (e.g. Anderson *et al.*, 2005), for *Dinophysis acuminata* (Raine *et al.*, 2010) and *Dinophysis acuta* (Farrell *et al.*, 2012) in coastal waters off the southern coast of Ireland and for *Pseudo-nitzschia* in the Northwest Pacific (Giddings *et al.*, 2014). Directional dispersal might be expected to yield sequential blooms of planktonic taxa if local blooms initiate in a location and then spread from that location primarily as a consequence of dispersal through water movement. Conversely, if local

blooms arise largely from highly localized processes acting on seed populations that are continuously present at all sites, then blooms in different local environments might not be expected to be sequential, but more random in appearance along the coast, unless the conditions favoring a species also appear sequentially at various locales [e.g. south-to-north (S-to-N) progression of seasonal warming, water stratification, etc.].

This study investigated the appearance of common HAB taxa at four piers within the Southern California Bight. Statistical analyses were performed in an effort to determine potential dependencies between algal species and environmental factors and to elucidate whether the appearance and dominance of HAB species arose as independent events at the various sampling sites or appeared first at a single location and in turn acted as "seed populations" for adjacent regions via local hydrography and currents. The analysis was accompanied by a simulation study in which Lagrangian particles were released in a Regional Ocean Model System in order to assess typical travel times between the piers.

METHOD

Sampling area

The Southern California Bight extends for ~700 km along the lower portion of the coast of California, from Point Conception to Cabo Colnett, Mexico. There is a rich history of the study of phytoplankton assemblages in the region, outlining the basic oceanographic features controlling primary production (Cullen and Eppley, 1981; Eppley *et al.*, 1985; Hickey, 1992). Circulation in the bight is complex and is affected by the California Current, a boundary current of the eastern North Pacific that moves southward along the continental coast, leading to northward-moving currents (California Countercurrent and California Undercurrent) that are induced by circulation and especially eddies formed off the shoreward side of the California Current. Wind forcing (both seasonally changing winds that blow north-to-south (N-to-S) alongshore and occasionally onshore-to-offshore) and physical impediments to these flows presented by the Channel Islands also contribute to complex circulation in the bight.

These features give rise to counterclockwise eddies of varying sizes and velocities, as well as seasonal upwelling along the coast (usually in winter and early spring), that affect water movement and phytoplankton production in the bight. Eddies cause significant lateral water movement within the bight, while upwelling-favorable winds transport surface waters seaward, resulting in the injection of nutrient-rich waters into the surface waters close to the coast. In addition, portions of the bight are influenced by inputs of anthropogenic nutrients resulting from major discharges from water treatment facilities in the region, as well as three highly channelized rivers (Santa Ana, Los Angeles and San Gabriel Rivers). These inputs contribute a substantial portion of the total nutrient loading of coastal waters in the bight. Locally (e.g. on the San Pedro shelf), these anthropogenically derived or influenced sources can deliver nutrient loads of the same magnitude as natural sources of nutrients contributed by upwelling of nutrient-rich deep waters (Howard *et al.*, 2014).

Data collection

All data were obtained from the SCCOOS (downloaded in March 2013 from http://www.sccoos.org). Data were collected at four shore stations along the coast of Southern California [Goleta Pier (GP), SW, Santa Monica Pier (SMP) and Newport Pier (NP, Table I and Fig. 1)], covering ~250 km of coastline between GP and NP. Sampling

Table I: Sampling location (latitude and longitude), monitoring period in which weekly samples were taken, number of data points analyzed in this period, range of chlorophyll a *(Chl.* a*), nitrate (N), phosphate (P) and domoic acid (DA) concentrations and ranges of water temperature for the four different sampling stations*

Sampling station	Sampling location (lat./long.)	Monitoring period	No. of data points	Chl. *a* (μg/L)	N (μM)	P (μM)	DA (μg/L)	Water temp. (°C)
Goleta Pier	34° 24.97′ N 119° 49.72′ W	12/13/2008 – 09/26/2011	122	0.0–16.8	0.02–21.58	0.27–1.90	0–6.6	11–21
Stearns Wharf	34° 24.48′ N 119° 41.10′ W	06/30/2008 – 12/17/2012	236	0.2–19.2	0.01–23.90	0.13–2.35	0–9.3	10–21
Santa Monica Pier	34° 0.48′ N 118° 29.94′ W	06/30/2008 – 08/20/2012	220	0.2–42.1	0.03–12.53	0.14–2.35	0–1.5	12–23
Newport Pier	33° 36.37′ N 117° 55.87′ W	06/30/2008 – 01/22/2013	228	0.1–37.2	0.15–13.19	0.11–1.82	0–3.0	11–24

The maximum number of available data points for each observable can differ for the same monitoring period because of recording gaps.

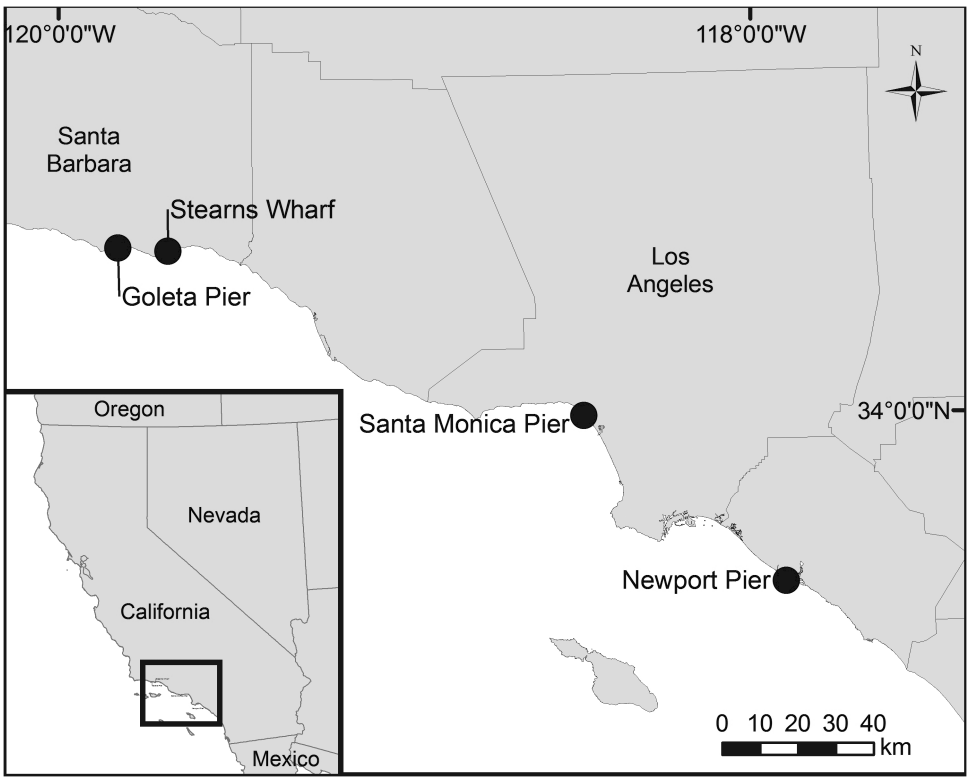

Fig. 1. Location of the SCCOOS weekly HAB monitoring piers in southern California, North American west coast, chosen for analysis and maintained through a collaboration of five university laboratories, beginning in June 2008.

started in June 2008 for all piers except for GP (December 2008) at a mean sampling interval Δt of 1 week, resulting in 122–236 data points per sampling station (Table I).

Methodology for sample collection and processing was standardized across the sampling sites. Briefly, samples were collected weekly on the same day of the week at each pier from surface waters using a clean bucket. Temperature was measured using a hand-held thermometer. Samples for the analysis of phytoplankton abundance and species composition were preserved and counted by inverted compound microscopy using the Utermöhl technique (Utermöhl, 1958). Dominant phytoplankton taxa were recorded and quantified from each sample, particularly HAB species (discussed subsequently). The concentration of chlorophyll *a* in each sample was determined fluorometrically from samples filtered onto GF/F glass fiber filters (Whatman) and extracted overnight in 100% acetone at −20°C in the dark (Parsons *et al.*, 1984). Domoic acid present in the plankton was assessed by enzyme-linked immunosorbent assay of the particulate material filtered onto glass fiber filters (Schnetzer *et al.*, 2013). Samples for dissolved inorganic nutrients (nitrite + nitrate, ammonium, phosphate and silicate) were collected and sent for analysis to the Marine Science Institute at the University of California Santa Barbara. Not all analyses were available for all sampling sites or dates.

In our analyses, we considered time series of abundances of different phytoplankton taxa, including *Akashiwo sanguinea*, *Alexandrium* spp., *Dinophysis* spp., *L. polyedrum*, *Prorocentrum* spp., *Pseudo-nitzschia* spp. (*seriata* size class) and *Pseudo-nitzschia* spp. (*delicatissima* size class). The latter two identifications each include a cluster of morphologically similar species (*sensu lato* Seubert *et al.*, 2013), herein referred to as *Pseudo-nitzschia seriata* and *Pseudo-nitzschia delicatissima*, respectively. We also included chlorophyll *a* as a proxy for total algal biomass and inorganic nutrients and temperature as abiotic factors.

We restricted our analyses to four sampling stations (SW, GP, SMP and NP), as these stations occurred within an area that matched the area of a simulation study of ocean currents by Mitarai *et al.* (2009), to which we compared our results in order to link spatial current patterns and current velocities to the occurrences and bloom events of particular algae; that is, to understand spatiotemporal dynamics of algal abundances (discussed subsequently).

Data processing

Time series of all factors were visually inspected. An outlier from the phosphate time series (occurring 30 August 2010) at SMP was identified and removed prior to subsequent

steps of analysis. In cases for which two samples of chlorophyll were taken at the same time and same station, we calculated the average of the samples.

Statistical analysis

We estimated kernel-based cross-correlation functions (CCFs) in order to assess dependencies between time series (see Supplementary data A for details about the estimation of CCFs and the statistical testing). As the size of the data set was limited, we reduced the number of statistical tests to achieve more statistical power (Futschik and Posch, 2005; Goeman and Solari, 2014): we restricted the statistical testing to mutual relationships between abundances of each taxa at different stations and to relationships between abundances of taxa and concentrations of nutrients (nitrate and phosphate) at each single station. More specifically, our statistical tests addressed the following questions. (i) Do abundances of a certain taxa at some station A tend to precede abundances of the same taxa at another station B? (ii) Do high concentrations of nutrients (nitrate or phosphate) at a station tend to co-occur with or to precede abundances of a certain taxa at the same station?

To address question (i), we carried out statistical tests for which we hypothesized that abundances at station A (B) could precede abundances at station B (A) up to 3 months. Taking into account all combinations of sampling stations (A, B), all studied algae taxa and both possible orders of temporal occurrence (A $\rightarrow$B, B $\rightarrow$A), 84 statistical tests were performed. To address question (ii), we hypothesized that nutrients could occur instantaneously or precede abundances of algal taxa by up to 3 weeks. Taking into account the number of taxa, sampling stations and nutrients, 56 statistical tests were carried out.

Carrying out multiple statistical tests (we considered 140 statistical tests in total) goes hand in hand with the problem of multiple comparisons: briefly, the more hypotheses that are tested, the larger the probability that at least one of them will erroneously be found to be true (a false positive finding, Goeman and Solari, 2014). To account for this effect, we controlled the false discovery rate (FDR), which is a widely used technique (FDR, Benjamini and Hochberg, 1995; Benjamini and Yekutieli, 2001). The FDR is the fraction of the expected number of false positive findings divided by the number of all positive findings. Throughout this article, we used FDR = 0.15, i.e. 15% of positive findings can be expected to be false positives.

For each dependency, which was significant according to our statistical tests, we identified the time lag associated with the maximum value (peak) of the respective CCF. To assess the significance of these peaks, we estimated the probabilities (*P*-values) to obtain larger values than the observed maximum values of the CCFs, given a suitable null model (see Supplementary data A for details).

Our statistical analysis was complemented with CCFs, which we determined between water temperature at different stations, between concentrations of nutrients (nitrate or phosphate) at different stations as well as between nutrients and chlorophyll (the latter as a proxy for total algal biomass) at each station.

Cross-correlation functions

In order to facilitate the interpretation of results of our time series analysis given subsequently, Fig. 2 shows an example time series of abundances of *L. polyedrum* sampled at GP and SMP (Fig. 2a) and the associated CCF (Fig. 2b). Major bloom events of this dinoflagellate with large amplitudes in autumn 2009 and summer 2010 were clearly apparent. The corresponding CCF (Fig. 2b; determined as detailed in the Method section and Supplementary data A) revealed the dependence of correlation (*y*-axis) between the two time series data sets, with a temporal shift (*x*-axis) between the two data sets. In this example, if the time series is not temporally shifted from one another (lag 0), the correlation between time series, and thus the value of the CCF, is small [CCF(0) = 0.13]. However, if the SMP time series is shifted by roughly 3 weeks to the right (positive lags), then major bloom events in both time series are superimposed and the correlation is large [CCF(24) = 0.90 for a shift of 24 days; numbers next to peaks in the CCF in Fig. 2b denote the associated time lag in days]. The analysis indicates that similar events in the time series of *L. polyedrum* sampled at SMP occurred ~3 weeks earlier than those in the time series sampled at GP. Another example (Fig. 2c and d) is shown for the time series of *Prorocentrum* spp. sampled at SMP and NP. When the NP time series was shifted to the left (negative lags) by roughly 50 days, the correlation was large [CCF(−52) = 0.65 at a lag of −52 days], indicating that bloom events in the time series of *Prorocentrum* spp. at SMP occurred ~52 days earlier than those in the time series at NP. In summary, peaks associated with negative lags indicate that events in the first time series preceded the ones of the second time series, whereas peaks associated with positive lags indicate that events in the second time series preceded the ones of the first time series ("first" and "second" refer to the ordering in the legends of Fig. 2a and c).

Lagrangian particle simulation

In order to gain more insights into potential travel times of water parcels within the bight, we conducted simulation studies. Simulated velocity fields of the ocean surface were obtained from the model output of a Regional Ocean Modeling System provided by the Central and Northern California Ocean Observing System. The

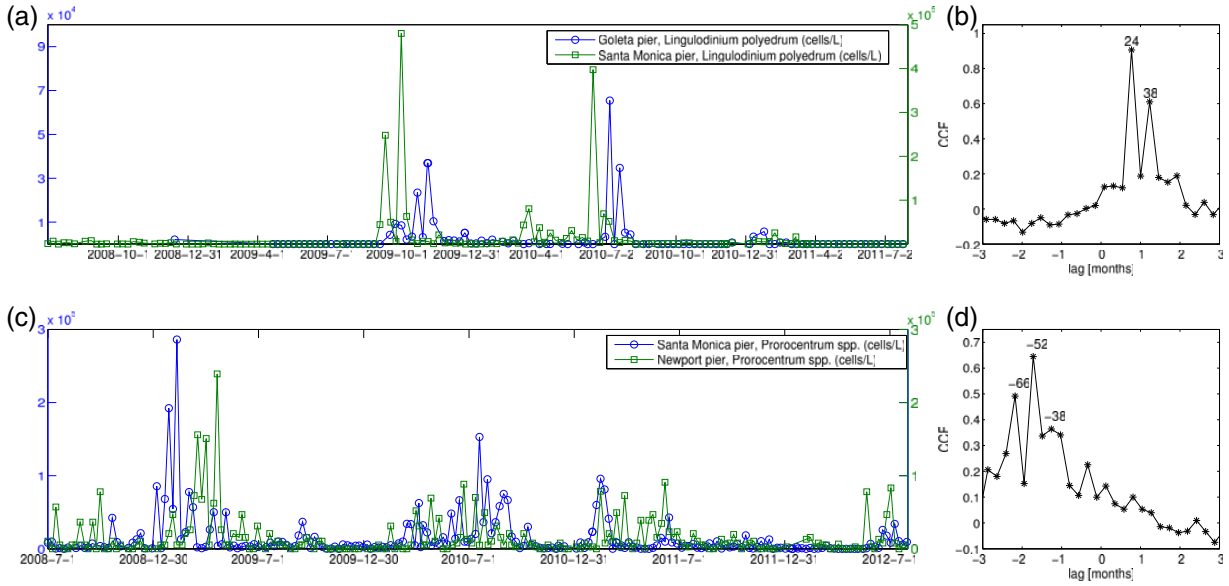

Fig. 2. Example time series of *L. polyedrum* at GP and SMP (**a**) and their CCF (**b**). Time series of *Prorocentrum* spp. at SMP and NP are shown in (**c**) as well as their corresponding CCF (**d**). Numbers next to peaks in (b) and (d) denote associated time lags (in days).

model is operated by UCLA and Remote Sensing Solutions, and its domain extends geographically from north of the California–Oregon border to south of the Mexican border (details about the model and the simulation are provided in Supplementary Data B). One thousand Lagrangian particles were released at random positions within a circle of 10 km radius in front of SMP every 12 h from 1 April 2013 till 1 April 2015. The positions of the Lagrangian particles were tracked for 100 days or until they left the simulated region. We defined target regions to be circles of 10 km radius in front of GP and NP. As soon as a particle released at SMP entered a target region for the first time, we recorded its travel time. Furthermore, Lagrangian particles released at SMP were grouped according to the season (spring, summer, autumn and winter).

RESULTS

Environmental conditions

The range of water temperatures observed throughout the study period was similar across the different stations (10–24°C). Maximum chlorophyll concentrations were approximately twice as high at SMP and NP (37–42 mg/m^3) than at SW and GP (17–19 mg/m^3), whereas domoic acid concentrations were highest at SW (9 ng/mL) and lowest at SMP (1.5 ng/mL, Table I).

Maximum phosphate concentrations were similar across the four different stations (1.8–2.4 μmol/L), whereas maximum nitrate concentrations differed substantially and were almost twice as high at GP and SW (21.6 and 23.9 μmol/L, respectively) than at SMP and NP (12.5 and 13.2 μmol/L, respectively, Table I; Supplementary data, Fig. S2).

Seasonal and annual ranges of HAB taxa

Abundances of target HAB species were highly variable at all sampling locations over the entire study period (Supplementary data, Fig. S1). Approximate ranges of maximum abundances at different piers were as follows: *A. sanguinea*: $2–8 \times 10^4$ cells/L, *Alexandrium* spp.: $5 \times 10^3–3 \times 10^5$ cells/L, *L. polyedrum*: $7 \times 10^4–9 \times 10^5$ cells/L, *P. delicatissima*: $5 \times 10^5–6 \times 10^6$ cells/L, *Dinophysis* spp.: $3 \times 10^3–2 \times 10^4$ cells/L, *Prorocentrum* spp.: $2–9 \times 10^5$ cells/L and *P. seriata*: $2–3 \times 10^5$ cells/L (Supplementary data, Fig. S1). For the first four taxa mentioned earlier, maximum cell abundances over the entire study period were observed at NP, whereas maximum cell abundances of *Dinophysis* spp. and *Prorocentrum* spp. were observed at SW. Abundances of *P. seriata* did not differ dramatically among stations (Supplementary data, Fig. S1).

In general, diatoms of the genus *Pseudo-nitzschia* were more prominent in spring and summer, with particularly high peaks of *P. seriata* in 2011 at all pier locations and in 2012 at SW and NP. *P. delicatissima* showed a particularly high peak in abundances in summer 2011 at NP and smaller peaks at different times and stations (Supplementary data, Fig. S1). Dinoflagellates were more prominent in summer and autumn. Blooms of different taxa were common at all piers in summer and autumn of each year (mainly *Lingulodinium* and *Prorocentrum*), with particularly high

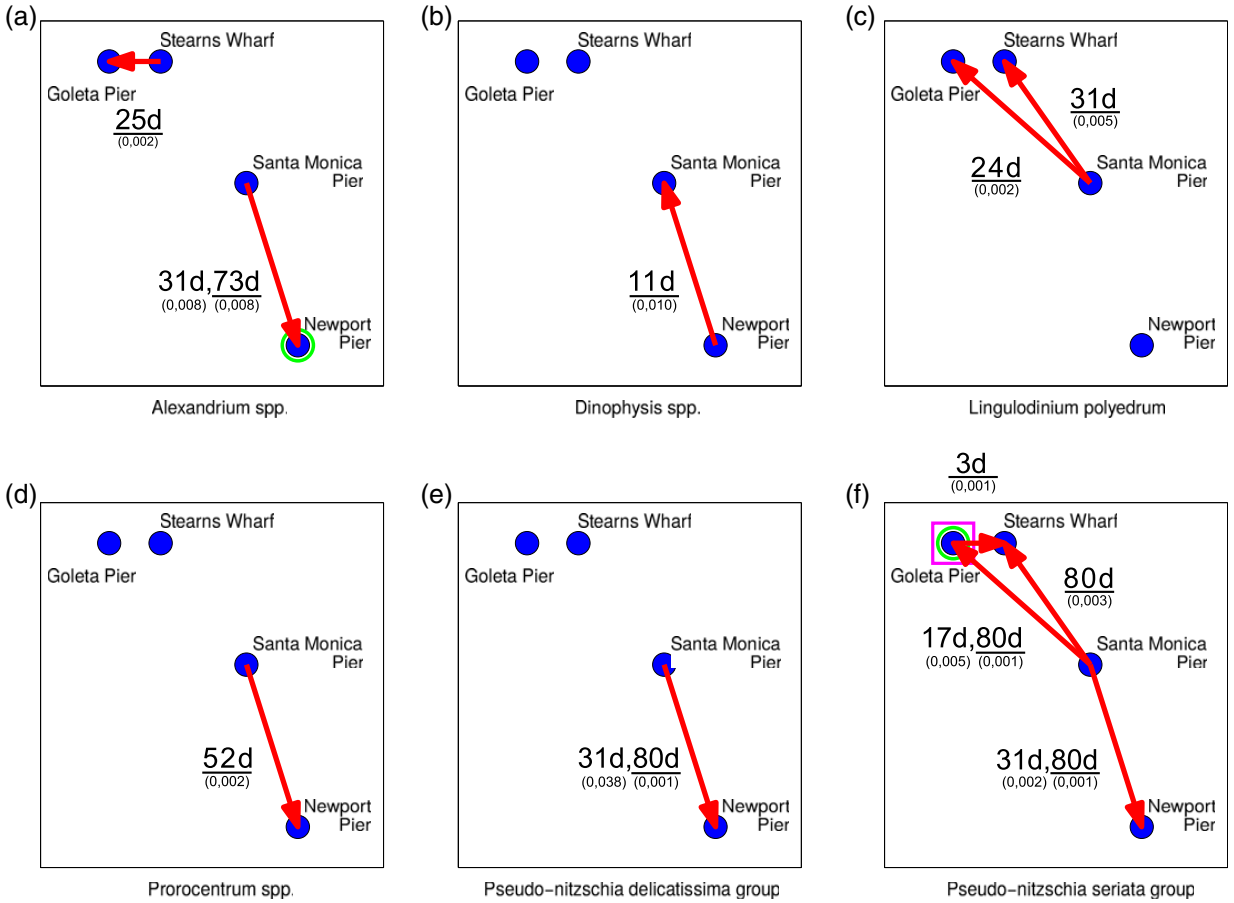

Fig. 3. Significant cross-correlations (arrows) between abundances of algal taxa at different stations (points): (**a**) *Alexandrium* spp., (**b**) *Dinophysis* spp., (**c**) *L. polyedrum*, (**d**) *Prorocentrum* spp., (**e**) *P. delicatissima*, (**f**) *P. seriata*. An arrow originating from one station and pointing to another station indicates that certain taxa occurred earlier at the former and later at the latter station. Numbers next to the arrows denote time lags (in days) associated with major peaks in the corresponding CCFs; numbers in parentheses are their associated *P*-values. Time lags of maximum values of the CCFs are underlined. Circles and rectangles denote significant cross-correlations between abundances of different taxa and nitrate [circles, nitrate precedes algal abundances by (**a**) 14 days and (**f**) 15 days) and phosphate [rectangle (f), phosphate precedes algal abundances by 18 days]. Positions of points (stations) in all panels do not correspond to geographical locations (cf. Fig. 1), but are arranged to enhance readability.

abundances at NP (Supplementary data, Fig. S1, except for *Prorocentrum*, see SW).

Spatiotemporal patterns of phytoplankton abundance

Significant dependencies of algal abundance among pier locations were detected for all algal taxa analyzed, except for *A. sanguinea* (Fig. 3). Different patterns of occurrence were observed for different algal taxa. For instance, *L. polyedrum* appeared earlier at SMP than at SW and GP (Fig. 3c, cf. Fig. 2a), with a time lag of roughly 31 and 24 days, respectively. A similar S-to-N pattern was observed for *P. seriata* between SMP and GP with time lags of ~17 and 80 days and between SMP and SW with a lag of ~80 days (Fig. 3f). An S-to-N pattern from NP to SMP was also observed for *Dinophysis* spp., with a time lag of 11 days (Fig. 3b). However, N-to-S relationships were observed for *P. seriata*, originating from SMP and subsequently showing peaks at NP with time lags of 31 and 80 days (Fig. 3f, cf. Fig. 4a). N-to-S patterns of appearance with similar time lags were also observed for *P. delicatissima* (Fig. 3e, cf. Fig. 4b), for *Alexandrium* spp. (31 and 73 days, Fig. 3a, cf. Fig. 4c) and for *Prorocentrum* spp. with a time lag of 52 days (Fig. 3d, cf. Fig. 2c).

Furthermore, significant relationships between the pier locations SW and GP occurred for *Alexandrium* spp. and *P. seriata* (Fig. 3a and f, respectively); however, these two pier locations are in close proximity (20 km) and therefore strong correlations in the appearance and abundances of algal taxa might be anticipated for these two sites. We did not observe any significant pattern indicating that an algal taxon occurred first at GP or SW and subsequently at any other station to the south.

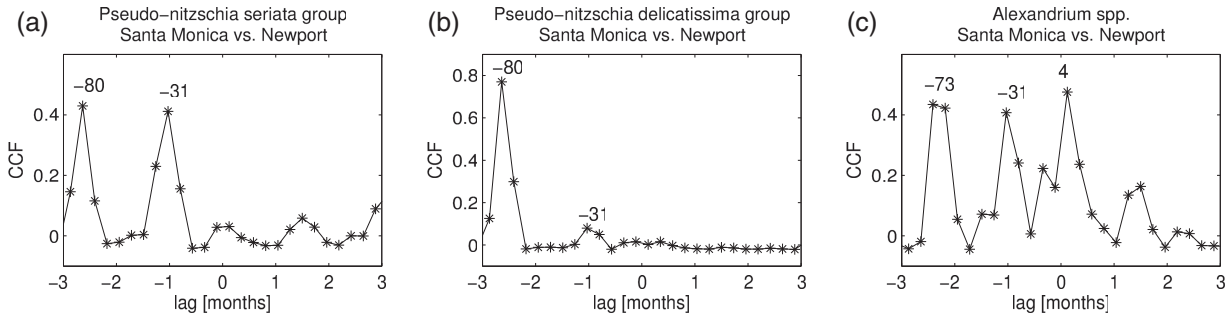

Fig. 4. CCF of (**a**) *P. seriata* size class, (**b**) *P. delicatissima* size class and (**c**) *Alexandrium* spp. between SMP and NP.

Environmental factors and phytoplankton taxa

Water temperature between the different stations was maximally correlated with zero time lag (Fig. 5a), indicating that seasonal temperature changes occurred simultaneously at all sampling stations (i.e. within the constraints of the frequency of sampling). CCFs further indicated that nitrate peaks occurred simultaneously at the different stations (Fig. 5b) and that increases in nitrate and phosphate concentrations occurred at the same time (Fig. 5c).

Investigating possible dependencies between dissolved nutrient concentrations (nitrate and phosphate) and algal taxa occurring locally at each station revealed that peaks of nitrate and phosphate occurred before peaks in *P. seriata* abundance at GP [Fig. 3f, time lags of 15 days for nitrate (see also Fig. 5e) and 18 days for phosphate], whereas high nitrate concentrations also preceded peaks in *Alexandrium* spp. abundance at NP (Figs 3a and 5d, time lag of 14 days). CCFs also revealed that nitrate preceded chlorophyll *a* by 7 days at NP (Fig. 5g); however, such a pattern could not be found for other stations (see, for instance, Fig. 5h).

Estimated travel times and trajectories for Lagrangian particles

In the simulation studies conducted, 7.5 and 7.3% of all particles released at SMP reached GP and NP, respectively. Histograms of particle travel times indicated that these travel times depend on the season (Fig. 6a and b). We observed variability in travel times within a season, ranging from a few days to several weeks.

The histogram of travel times between SMP and GP exhibited a bimodal structure for spring, displaying two broad peaks at ∼30 and 60 days. The first peak was in approximate agreement with spatiotemporal patterns of occurrences of *L. polyedrum* (Fig. 3c; travel times of 24 days from SMP to GP and 31 days to the nearby station SW) as estimated by the cross-correlation analysis. For *P. seriata*, on the contrary, we observed a double-peak structure in the CCFs, indicating the presence of two dominant time lags of 17 and 80 days (Fig. 3f). This mirrored the bimodal pattern present in the distribution of travel times in the histogram during spring (Fig. 6a). We note that the broad distributions of travel times present during summer and autumn would also explain the observation of lags as estimated by our cross-correlation analysis. Example trajectories of particles being advected from SMP to GP in our simulation study indicated that Lagrangian particles that reach GP after ∼30 days are typically advected along the coast northwards, whereas particles with much longer travel times tend to be entrained by eddies and traverse a larger region of the bight (Fig. 6c).

The histogram of travel times estimated for particles advected from SMP to NP indicated that particles typically needed 10–25 days to travel from SMP to NP during spring, summer and autumn (Fig. 6b). For spring, we observed an additional broad peak around 70 days. Such a double-peak structure was also reflected in dominant lags, as observed in our cross-correlation analysis for *Alexandrium* (Fig. 3a), *P. delicatissima* (Fig. 3e) and *P. seriata* (Fig. 3f). The particles corresponding to short travel times tended to remain near SMP for some time and were then advected directly along the coast to NP (Fig. 6d). In contrast, particles with longer travel times tended to be entrained in large-scale eddies in the Southern California Bight before they reached NP (Fig. 6d), in a similar way as was observed for the S-to-N movement from SMP to GP.

Seasonal variations were apparent when histograms of travel times from SMP to GP (S-to-N, Fig. 6a) and from SMP to NP (N-to-S, Fig. 6b) were compared. During spring, travel times of particles traveling to the north tended to be longer (Fig. 6a) than those traveling to the south (Fig. 6b). In contrast, during winter, travel times of particles traveling to the north (Fig. 6a) were shorter than those traveling to the south (Fig. 6b).

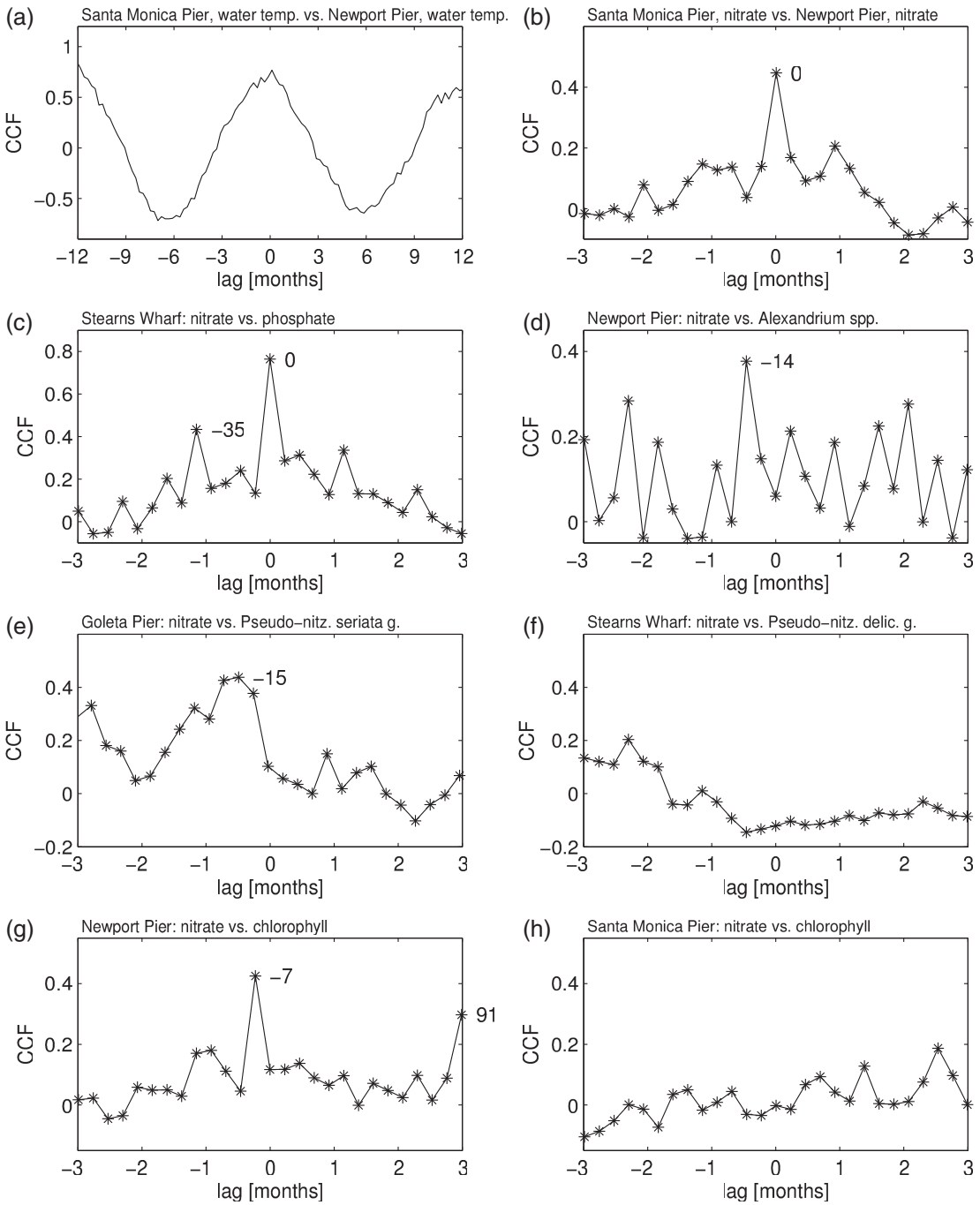

Fig. 5. CCF among various environmental factors and algal abundances at different stations. Numbers next to selected peaks are the corresponding time lags in days.

DISCUSSION

Our predictive understanding of the timing, location and species composition of phytoplankton blooms is limited because of the complex interactions among the many chemical and biological forcing factors that control these processes and populations. Local conditions (e.g. water temperature, nutrient availability, grazers, etc.) must certainly play a role in the success or failure of algal populations, but these interactions are further complicated by the potential for advection of populations or whole communities past a fixed sampling point (a Eulerian sampling approach). The CCFs employed in this study to investigate

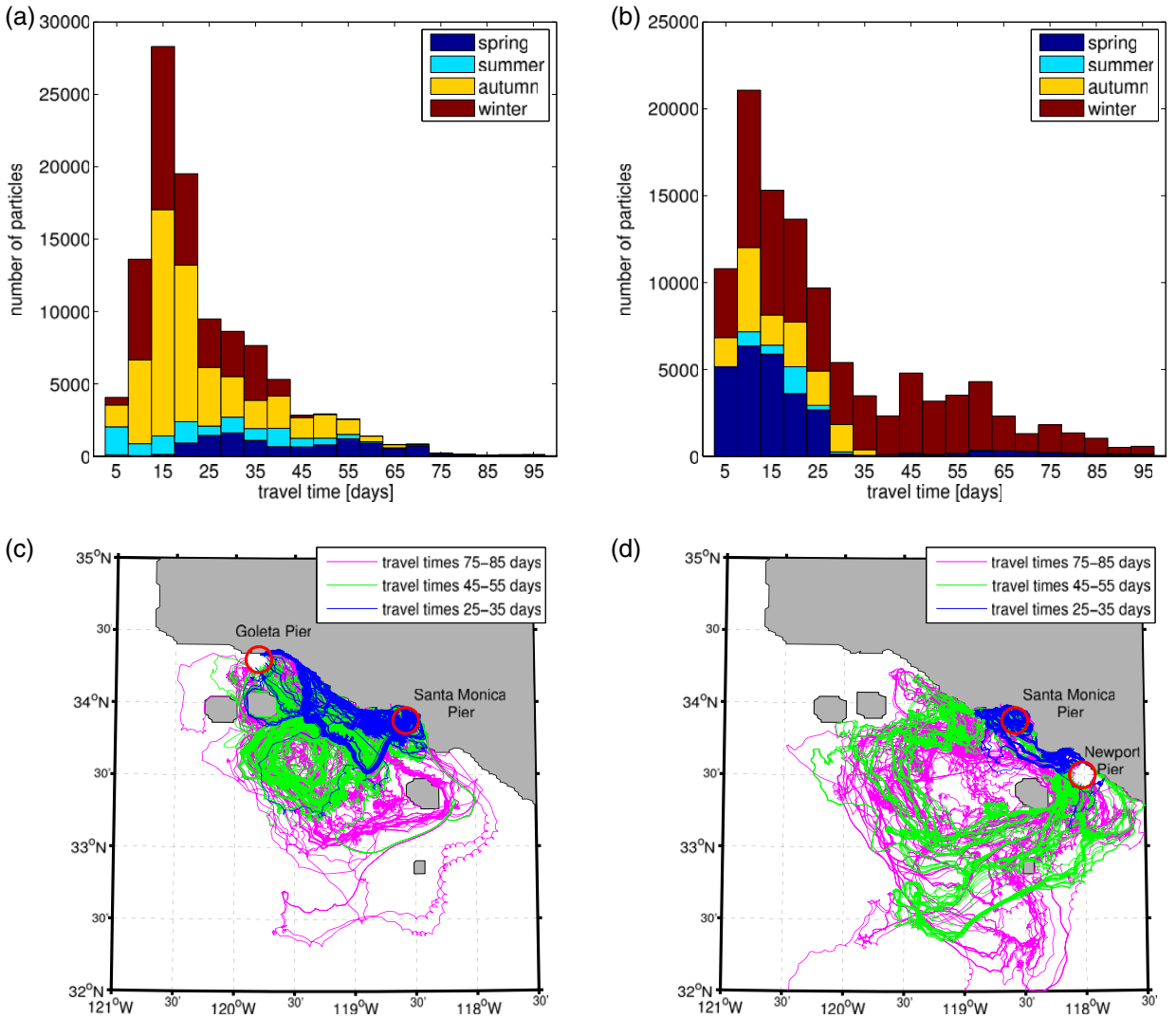

Fig. 6. Histograms of travel times estimated for Lagrangian particles released at SMP and reaching GP (**a**) and NP (**b**), respectively. Particles and their travel times are distinguished according to the season during which they were released at SMP. Example trajectories of particles released during spring and reaching GP (**c**) and NP (**d**). Visualized trajectories belong to travel times of 25–35 days, 45–55 days and 75–85 days. Release and target sites are shown as circles.

spatiotemporal dynamics of different phytoplankton species and potential interdependencies of these species with environmental factors revealed a number of different correlations among the HAB-forming species within the Southern California Bight that helped to identify a number of these complexities.

A variety of factors undoubtedly contributed to the observed patterns and corresponding time lags of bloom dynamics. For instance, spatial patterns of occurrences could be due to similar hydrographic conditions arising in a temporal sequence at different locales. An S-to-N pattern might be expected from a yearly up-coast progression of spring. If such seasonality were the reason for the observed temporal sequences of blooms, one would expect seasonality-related environmental factors to also show similar temporal lags between stations as observed for the algal species. As a proxy for latitudinally related seasonality, we analyzed water temperature at the four stations using CCFs. However, temperatures between all pairs of stations were correlated with zero lag (Fig. 5a), indicating that the spatial distances and temporal resolution of 1 week were too small to clearly identify any south (S) to north (N) seasonal increase in temperature that might explain the S-to-N propagation of some algal taxa observed in our data. These findings may reflect the fact that the Southern California Bight is not large latitudinally (≈700 km) and thus subject to relatively uniform seasonality. It may also reflect that the region is located at the border of temperate/subtropical latitudes, where annual

temperature fluctuations are modest (typically $<5^{\circ}$C) and therefore of little direct importance for phytoplankton population growth, relative to communities at higher latitude. This aspect is supported by a study of Kim *et al.* (2009), who did not find any correlation between monthly averaged nearshore chlorophyll *a* and temperature, wind or climate indices when analyzing a 20-year record of chlorophyll *a* from the Scripps Pier, La Jolla, California. Therefore, some of the factors that control phytoplankton blooms in temperate regions (such as temperature) may not play dominant roles in this system.

Episodic coastal upwelling events are an alternative explanation for the observed spatial patterns and time lags in the appearance of HAB species. Upwelling events have been identified as factors correlating toxic blooms of *Pseudo-nitzschia* and other algal blooms in California coastal waters (Trainer *et al.*, 2000; Kudela *et al.*, 2005; Anderson *et al.*, 2006; Lane *et al.*, 2010; Omand *et al.*, 2012; Schnetzer *et al.*, 2013). The upward vertical flux of nitrate into the euphotic zone resulting from upwelling is widely believed to be a critical control of phytoplankton growth in this context (Eppley *et al.*, 1979; Omand *et al.*, 2012) and may act to seed surface communities of phytoplankton with cells from subsurface depths in the euphotic zone (Seegers *et al.*, 2015). In our study, nitrate peaks appeared simultaneously at different stations (Fig. 5b and Supplementary data, Fig. S2), indicating that upwelling events were bight-wide phenomena [an observation also reported in previous studies, see Anderson *et al.* (2008) and Nezlin *et al.* (2012)], in which case they could not explain the time lags observed for the sequential occurrences of algal taxa along the coast. Moreover, bight-wide upwelling events would contribute to zero lag correlations of temperature between stations, which is consistent with our observations (Fig. 5a). For some taxa and stations, peaks in nitrate preceded peaks in algal abundance, such as *Alexandrium* spp. at NP and *P. seriata* at GP (Fig. 5d and e). In these cases, upwelling might indeed have been a reason for the local occurrence of these algae. A nitrate peak preceding a chlorophyll *a* peak (proxy for total algal biomass) by 7 days at NP (Fig. 5g) was a further indication for such a local phenomenon. Similarly, Omand *et al.* (2012) found that a nitrate flux event preceded each of three distinct bloom events between mid-June and mid-October in 2006 at Huntington Beach, CA, one of which was a *L. polyedrum* bloom, and suggested that the blooms were a response to these fluxes. Likewise, Nezlin *et al.* (2012) investigated 38 upwelling events and reported increased chlorophyll concentrations after 5–8 days at several locations within the SCB and up to 15 days along the Central Coast.

Significant dependencies of algal abundances among pier locations indicated significant spatiotemporal relationships for five out of the six algal taxa studied. Interestingly, the N-to-S and S-to-N sequential appearance of taxa was approximately equal. Almost all of them occurred first at SMP and, after a certain time lag, either north (SW and GP; *L. polyedrum* and *P. seriata*) or south (NP; *Alexandrium*, *Prorocentrum*, both *Pseudo-nitzschia* size classes) of SMP. The only exception was *Dinophysis*, for which an S-to-N pattern was observed from NP to SMP.

We compared our results with those obtained from a simulation study of ocean currents (Mitarai *et al.*, 2009) in order to shed more light on the spatiotemporal dynamics of the occurrences of algal taxa; that is, the time lags of their peaks in abundances at different stations determined from our analysis. The study of Mitarai *et al.* (2009) investigated the probability that parcels of water are transported from one location to another location via currents in the Southern California Bight over a specified time interval. Probabilities were obtained by releasing Lagrangian particles at different locales and times in the model and tracking their location due to passive transport by simulated ocean currents. Although the time span (years 1996–2002) of this simulation does not match our observation period, we reasoned that the study, nevertheless, might provide clues about the average transport patterns of algal assemblages observed in the Southern California Bight due to ocean currents.

On the basis of the results of the simulation study, we inferred that SW and GP were not good sources but a good destination for water parcels from other parts of the coast [cf. Figs 8a and 9a in Mitarai *et al.* (2009)]. The results of our CCF analysis agree with observational and simulation current data because dependencies pointed from SMP to GP and SW in the north, but not vice versa (cf. Fig. 3). Furthermore, the simulation study identified the coastal area of SMP and NP as good sources as well as good destinations of water parcels. This also agrees with our CCF findings, which indicated that SMP was a particularly good source for algae (cf. Fig. 3, most arrows originated there), which first increased in abundance at SMP and then subsequently in the north (GP and SW) or south (NP, mentioned earlier). NP was thus more a destination point in our study, with the exception of *Dinophysis*, which first occurred at NP and later at SMP.

The simulation study of Mitarai *et al.* (2009) also estimated average transport times of water parcels released in the southern part of the bight at Oceanside ($\sim$75 km south of NP) to other locations northward along the coast (cf. Fig. 16c in Mitarai *et al.*, 2009). If we assume that transport by currents occurred near the coast from S-to-N, we can deduce from this figure an estimated average transport time of $\sim$10 days from NP to SMP and of 20–30 days from SMP to SW and GP. These values are generally in agreement with the identified time lags

for *Dinophysis* spp. from NP to SMP (11 days), for *L. polyedrum* from SMP to SW and GP (~24 and 31 days) and for *P. seriata* (from SMP to GP, 17 days). We note that, for the majority of taxa, our study indicated transport from SMP to NP (Fig. 3, discussed subsequently); therefore, it is likely that an N-to-S movement observed from SMP to NP was a consequence of transport, whereas other factors such as local environmental conditions that we did not assess in our study might have contributed to the patterns observed for *Dinophysis*. For *L. polyedrum*, observed cell abundances were generally higher at SMP first than later at GP (cf. Fig. 2a). This temporal pattern of abundances at the two sites may be a consequence of populations that are distributed by ocean currents. The filamentous nature of coastal eddies may have transported patches of algae with them, diluting the abundances of blooms as they are transported from one locale to another. Such thinning could have happened in our case during a hypothetical transport to the north. A similar phenomenon of decreasing abundances due to transport has been described in the Benguela upwelling region (Hernandez-Carrasco *et al.*, 2014). In contrast, seasonal forcing was reported to be the reason for an S-to-N pattern of occurrence of *A. fundyense* in the Gulf of Maine, a temporal pattern in the opposite direction of the coastal current (McGillicuddy *et al.*, 2005). Even though some of our results match the current patterns simulated by Mitarai *et al.* (2009), travel times between our four stations were only estimated visually from their results, and their findings were obtained by analyzing a time period (1996–2002) that was different from the sampling period we analyzed. That study also used a different release site (Oceanside south of NP). Hence, in order to more accurately predict algal transport by currents in our study area, we conducted simulation studies releasing and tracking Lagrangian particles at SMP (see Method and Supplementary Data B). These simulations of the advection of particles by prevailing ocean currents in the bight supported our findings.

In spring, travel times between SMP and GP of ~30 and 60 days were observed in our simulations (cf. Fig. 6a). The first peak corresponds to spatiotemporal patterns of occurrences of *L. polyedrum* as estimated by the cross-correlation analysis, whereas the double-peak structure mirrors the observed time lags of 17 and 80 days in the CFF for *P. seriata*.

Similarly, a double-peak structure in travel times was observed from SMP to NP during spring in our simulations (10–30 and 70 days, cf. Fig. 6b), reflected in dominant lags observed in our cross-correlation analysis for *Alexandrium*, *P. delicatissima* and *P. seriata*.

In general, meso- and submesoscale hydrodynamic structures such as eddies have been shown to be essential determinants of biological growth (Martin *et al.*, 2002; D'Ovidio *et al.*, 2010; Levy *et al.*, 2012), but such analyses are to the best of our knowledge still lacking for the California Bight. A major bloom event of *P. delicatissima* and *P. seriata* occurred at SMP on 14 March 2011 and just 1 week earlier a bloom of *Alexandrium* spp. These three taxa occurred at NP 31 and 73–80 days later. Such a pattern is consistent with two different routes plankton patches can take starting from SMP and reaching NP. According to studies by Dong *et al.* (2009, cf. upper left panels in Figs 6 and 14 therein), there is a direct route to NP which could correspond to the short travel time, but also a longer route involving two vortices of ca. 50 km diameter each which could be related to the long travel time. Plankton that are entrained by mesoscale vortices have significantly enhanced travel times (Sandulescu *et al.*, 2007; Bastine and Feudel, 2010; D'Ovidio *et al.*, 2013). If some fraction of an algal population were enclosed by a vortex and the other fraction not, the fraction outside of the vortex would arrive faster at the destination compared with the enclosed fraction, which would be transported with the slower mean velocity of the vortex. Our simulation study supports that idea; trajectories of particles being advected from SMP to NP indicate that particles corresponding to short travel times tend to stay around SMP for a while before being directly advected along the coast to NP, whereas particles with longer travel times tend to be entrained in large-scale eddies before they reach NP. Similarly, Lagrangian particles which reach GP after ~30 days are typically advected along the coast northwards, and particles with much longer travel times are likely to be entrained by eddies and traverse a larger region of the bight.

However, seasonal variations of these patterns become apparent when comparing travel times from SMP to GP (S-to-N) and from SMP to NP (N-to-S). During spring, travel times of particles traveling to the north tend to be longer than those traveling to the south and vice versa in winter (cf. Fig. 6a and b). This agrees with what is known about the seasonal variations of gross circulation patterns within the bight [see Bray *et al* (1999) as well as references therein; Hickey, 1992]. During winter, the California counter current (Davidson current) is the dominant surface current at the coast, transporting warm waters from south to north and through the Santa Barbara channel as well as south of the Channel Islands. We observed the histogram of travel times during winter to show longer travel times for particles advected southwards and thus to the opposite direction of the Davidson current than for particles advected northwards and thus along the Davidson current. This picture changes during spring where the Davidson current weakens at the surface [while still being present as California Undercurrent at ~100–300 m below the surface (Hickey, 1992)]. At the same time, the California

current, which transports cold waters offshore from north to south, moves closer to the shore, effectively reversing the direction of the current at the coast which now predominantly points to the south. Indeed, travel times of particles released during spring and advected to the south show a tendency toward shorter travel times than those being advected to the north (cf. Fig. 6a and b).

In addition to seasonal dynamics, hydrodynamic flow patterns in the California Bight can be rather different from year to year. Regions that serve as sources for tracers in one year can become destinations for particles in another year (Watson *et al.*, 2010).

This study provides evidence that hydrodynamic transport is an important factor for the spatiotemporal patterns of occurrences of HAB. However, we are aware of a number of limitations of this contribution. Although the identified time lags between stations revealed by the cross-correlation analyses are in approximate agreement with mean travel times as reported in Mitarai *et al.* (2009) and as estimated in our Lagrangian particle simulations, the data sets underlying these results cover different and non-overlapping time periods. Although these different data sources support a coherent picture, this introduces some uncertainty in our interpretation. In addition, the Lagrangian particle simulation does not take into account a possible diurnal vertical migration of phytoplankton, such as demonstrated for many dinoflagellates (e.g. Blasco, 1978; Eppley *et al.*, 1984), which could affect hydrodynamic transport as cells may encounter different velocity fields depending on their location in the vertical water column. Indeed, vertical migration may affect transportation patterns as exemplarily demonstrated for zooplankton transport (Carr *et al.*, 2008). Finally, the observed time lags between the occurrences of taxa at different stations as well as typical travel times of hydrodynamic transport (as observed by the simulation study) within the Southern California Bight spanned several days to weeks. Typical time scales of algal population dynamics, which we did not consider in this contribution, will act on much shorter time scales. To gain a predictive understanding of the spatiotemporal patterns of occurrences of HABs, deeper insights into the complex interplay between hydrodynamics and population dynamics are necessary, for instance, by coupling monitoring data, simulation studies and biogeochemical models. This promising approach has been used to investigate and to predict occurrence patterns of different algal species in various study regions (see review by Anderson *et al.*, 2015).

CONCLUSION

Overall, our time-series analysis emphasizes that spatiotemporal dynamics of HABs are determined by a variety of different factors, including hydrography and coastal upwelling events. Variations in local hydrological factors such as temperature or nutrient regime were not sufficient to allow prediction of the kind of algal bloom that would develop or its timing. Instead, complex physics in the Southern California Bight relating to ocean currents appeared to be important in determining the propagation of HABs, especially the regional transport of "seed populations" via ocean currents. Our results are promising and could motivate future work in which, for instance, Lagrangian particles are released exactly at those times and places where high abundances of algal cells are indeed observed (e.g. by the SCCOOS program), which could also provide a deeper understanding of spatial and seasonal variability of the occurrence of HAB. Combining monitoring data with hydrodynamic and biogeochemical models will be useful to enhance our predictive understanding of occurrence patterns of HABs.

SUPPLEMENTARY DATA

Supplementary data can be found online at http://plankt.oxfordjournals.org.

ACKNOWLEDGEMENTS

The authors would like to thank John McGowan and Melissa Carter for informal comments on earlier versions of this manuscript and all investigators and their staff and students associated with the Southern California Coastal Ocean Observing System Harmful Alga Blooms project.

FUNDING

This work was supported by the Volkswagen Foundation (Grant no. 85388, 85389, 85390, 88459, 88461, 88464) and National Oceanic and Atmospheric Administration grants NA08OAR4320894 and NA11NOS4780052.

REFERENCES

Allen, W. E. (1946) "Red water" in La Jolla Bay in 1945. *Trans. Am. Microsc. Soc.*, **65**, 262–264.

Anderson, C. R., Brzezinski, M. A., Washburn, L. and Kudela, R. (2006) Circulation and environmental conditions during a toxigenic *Pseudo-nitzschia australis* bloom in the Santa Barbara Channel, California. *Mar. Ecol. Prog. Ser.*, **327**, 119–133.

Anderson, C. R., Moore, S., Tomlinson, M., Silke, J. and Cusak, C. (2015) Living with harmful algal blooms in a changing world: strategies for modeling and mitigating their effects in coastal marine ecosystems. In Ellis, J. and Sherman, D. (eds), *Coastal and Marine Hazards, Risks, and Disasters*. Elsevier B.V., Amsterdam, pp. 495–561.

Anderson, C. R., Siegel, D. A., Brzezinski, M. A. and Guillocheau, N. (2008) Controls on temporal patterns in phytoplankton community structure in the Santa Barbara Channel, California. *J. Geophys. Res. Oceans*, **113**, C04038.

Anderson, D. M., Keafer, B. A., Geyer, W. R., Signell, R. P. and Loder, T. C. (2005) Toxic *Alexandrium* blooms in the western Gulf of Maine: the plume advection hypothesis revisited. *Limnol. Oceanogr.*, **50**, 328–345.

Bastine, D. and Feudel, U. (2010) Inhomogeneous dominance patterns of competing phytoplankton groups in the wake of an island. *Nonlin. Process. Geophys.*, **17**, 715–731.

Benjamini, Y. and Hochberg, Y. (1995) Controlling the false discovery rate: a practical and powerful approach to multiple testing. *J. R. Stat. Soc. Ser. B*, **57**, 289–300.

Benjamini, Y. and Yekutieli, D. (2001) The control of the false discovery rate in multiple testing under dependency. *Ann. Stat.*, **29**, 1165–1188.

Blasco, D. (1978) Observations on the diel migration of marine dinoflagellates off the Baja California Coast. *Mar. Biol. (New York)*, **46**, 41–47.

Bray, N. A., Keyes, A. and Morawitz, W. M. L. (1999) The California Current system in the Southern California Bight and the Santa Barbara Channel. *J. Geophys. Res. Oceans*, **104**, 7695–7714.

Busse, L. B., Venrick, E. L., Antrobus, R., Miller, P. E., Vigilant, V., Silver, M. W., Mengelt, C., Mydlarz, L. *et al.* (2006) Domoic acid in phytoplankton and fish in San Diego, CA, USA. *Harmful Algae*, **5**, 91–101.

Caron, D. A., Garneau, M.-È., Seubert, E., Howard, M. D. A., Darjany, L., Schnetzer, A., Cetinić, I., Filteau, G. *et al.* (2010) Harmful algae and their potential impacts on desalination operations off southern California. *Water Res.*, **44**, 385–416.

Carr, S. D., Capet, X. J., McWilliams, J. C., Pennington, J. T. and Chavez, F. P. (2008) The influence of diel vertical migration on zooplankton transport and recruitment in an upwelling region: estimates from a coupled behavioral-physical model. *Fish. Oceanogr.*, **17**, 1–15.

Cullen, J. J. and Eppley, R. W. (1981) Chlorophyll maximum layers of the Southern-California Bight and possible mechanisms of their formation and maintenance. *Oceanol. Acta*, **4**, 23–32.

D'Ovidio, F., De Monte, S., Alvain, S., Dandonneau, Y. and Levy, M. (2010) Fluid dynamical niches of phytoplankton types. *Proc. Natl Acad. Sci. USA*, **107**, 18366–18370.

D'Ovidio, F., De Monte, S., Penna, A. D., Cotte, C. and Guinet, C. (2013) Ecological implications of eddy retention in the open ocean: a Lagrangian approach. *J. Phys. A: Math. Theor.*, **46**, 254023.

Dong, C., Idica, E. Y. and McWilliams, J. C. (2009) Circulation and multiple-scale variability in the Southern California Bight. *Progress in Oceanography*, **82**, 168–190.

Eppley, R. W., Reid, F. M. H., Cullen, J. J., Winant, C. D. and Stewart, E. (1984) Subsurface patch of a dinoflagellate (*Ceratium tripos*) off Southern California: patch length, growth rate, associated vertically migrating species. *Mar. Biol. (New York)*, **80**, 207–214.

Eppley, R. W., Renger, E. H. and Harrison, W. G. (1979) Nitrate and phytoplankton production in Southern California coastal waters. *Limnol. Oceanogr.*, **24**, 483–494.

Eppley, R. W., Stewart, E., Abbott, M. R. and Heyman, U. (1985) Estimating ocean primary production from satellite chlorophyll. Introduction to regional differences and statistics for the Southern California Bight. *J. Plankton Res.*, **7**, 57–70.

Farrell, H., Gentien, P., Fernand, L., Lunven, M., Reguera, B., González-Gil, S. and Raine, R. (2012) Scales characterising a high density thin layer of *Dinophysis acuta* Ehrenberg and its transport within a coastal jet. *Harmful Algae*, **15**, 36–46.

Franks, P. J. S. and Anderson, D. M. (1992a) Alongshore transport of a toxic phytoplankton bloom in a buoyancy current: *Alexandrium tamarense* in the Gulf of Maine. *Mar. Biol.*, **112**, 153–164.

Franks, P. J. S. and Anderson, D. M. (1992b) Toxic phytoplankton blooms in the southwestern Gulf of Maine: testing hypotheses of physical control using historical data. *Mar. Biol.*, **112**, 165–174.

Franks, P. J. S. and Keafer, B. A. (2003) Sampling techniques and strategies for coastal phytoplankton blooms. In Hallegraeff, G. M., Anderson, D. M. and Cembella, A. D. (eds), *Manual on Harmful Marine Microalgae*. Unesco, Paris, pp. 51–76.

Frolov, S., Kudela, R. M. and Bellingham, J. G. (2012) Monitoring of harmful algal blooms in the era of diminishing resources: a case study of the U.S. West Coast. *Harmful Algae*, **21–22**, 1–12.

Futschik, A. and Posch, M. (2005) On the optimum number of hypotheses to test when the number of observations is limited. *Stat. Sin.*, **15**, 841–855.

Garneau, M.-È., Schnetzer, A., Countway, P. D., Jones, A. C., Seubert, E. L. and Caron, D. A. (2011) Examination of the seasonal dynamics of the toxic dinoflagellate *Alexandrium catenella* at Redondo Beach, California, by quantitative PCR. *Appl. Environ. Microbiol.*, **77**, 7669–7680.

Giddings, S. N., Maccready, P., Hickey, B. M., Banas, N. S., Davis, K. A., Siedlecki, S. A., Trainer, V. L., Kudela, R. M. *et al.* (2014) Hindcasts of potential harmful algal bloom transport pathways on the Pacific Northwest coast. *J. Geophys. Res. Oceans*, **119**, 2439–2461.

Glibert, P. M., Allen, J. I., Bouwman, A. F., Brown, C. W., Flynn, K. J., Lewitus, A. J. and Madden, C. J. (2010) Modeling of HABs and eutrophication: status, advances, challenges. *J. Mar. Syst.*, **83**, 262–275.

Goeman, J. J. and Solari, A. (2014) Tutorial in biostatistics: multiple hypothesis testing in genomics. *Stat. Med.*, **33**, 1946–1978.

Gregorio, D. E. and Pieper, R. E. (2000) Investigations of red tides along the Southern California coast. *Bull. South. Calif. Acad. Sci.*, **993**, 147–160.

Heisler, J., Glibert, P. M., Burkholder, J. M., Anderson, D. M., Cochlan, W., Dennison, W. C., Dortch, Q., Gobler, C. J. *et al.* (2008) Eutrophication and harmful algal blooms: a scientific consensus. *Harmful Algae*, **8**, 3–13.

Hernandez-Carrasco, I., Rossi, V., Hernandez-Garcia, E., Garcon, V. and Lopez, C. (2014) The reduction of plankton biomass induced by mesoscale stirring: a modeling study in the Benguela upwelling. *Deep Sea Res. I*, **83**, 65–80.

Hickey, B. M. (1992) Circulation over the Santa Monica–San Pedro basin and shelf. *Prog. Oceanogr.*, **30**, 37–115.

Holmes, R. W., Williams, P. M. and Eppley, R. W. (1967) Red water in La Jolla Bay, 1964–1966. *Limnol. Oceanogr.*, **12**, 503–512.

Howard, M. D. A., Cochlan, W. P., Ladizinsky, N. and Kudela, R. M. (2007) Nitrogenous preference of toxigenic *Pseudo-nitzschia australis* (Bacillariophyceae) from field and laboratory experiments. *Harmful Algae*, **6**, 206–217.

Howard, M. D. A., Jones, A. C., Schnetzer, A., Countway, P. D., Tomas, C. R., Kudela, R. M., Hayashi, K., Chia, P. *et al.* (2012) Quantitative real-time polymerase chain reaction for *Cochlodinium fulvescens* (Dinophyceae), a harmful dinoflagellate from California coastal waters. *J. Phycol.*, **48**, 384–393.

Howard, M. D. A., Silver, M. and Kudela, R. M. (2008) Yessotoxin detected in mussel (*Mytilus californicus*) and phytoplankton samples from the U.S. west coast. *Harmful Algae*, **7**, 646–652.

Howard, M. D. A., Sutula, M., Caron, D. A., Chao, Y., Farrara, J. D., Frenzel, H., Jones, B., Robertson, G. *et al*. (2014) Anthropogenic nutrient sources rival natural sources on small scales in the coastal waters of the Southern California Bight. *Limnol. Oceanogr.*, **59**, 285–297.

Jessup, D. A., Miller, M. A., Ryan, J. P., Nevins, H. M., Kerkering, H. A., Mekebri, A., Crane, D. B., Johnson, T. A. *et al*. (2009) Mass stranding of marine birds caused by a surfactant-producing red tide. *PLoS ONE*, **4**, e4550.

Kim, H.-J., Miller, A. J., McGowan, J. and Carter, M. L. (2009) Coastal phytoplankton blooms in the Southern California Bight. *Prog Oceanogr.*, **82**, 137–147.

Kudela, R., Pitcher, G., Probyn, T., Figueiras, F., Moita, T. and Trainer, V. (2005) Harmful algal blooms in coastal upwelling systems. *Oceanography*, **18**, 184–197.

Lane, J. Q., Roddam, C. M., Langlois, G. W. and Kudela, R. M. (2010) Application of Solid Phase Adsorption Toxin Tracking (SPATT) for field detection of the hydrophilic phycotoxins domoic acid and saxitoxin in coastal California. *Limnol. Oceanogr. Methods*, **8**, 645–660.

Levy, M., Ferrari, R., Franks, P. J. S., Martin, A. P. and Riviere, P. (2012) Bringing physics to life at the submesoscale. *Geophys. Res. Lett.*, **39**, L14602

Lewitus, A. J., Horner, R. A., Caron, D. A., Garcia-Mendoza, E., Hickey, B. M., Hunter, M., Huppert, D. D., Kudela, R. M. *et al*. (2012) Harmful algal blooms along the North American west coast region: history, trends, causes, and impacts. *Harmful Algae*, **19**, 133–159.

Martin, A. P., Richards, K. J., Bracco, A. and Provencale, A. (2002) Patchy productivity in the open ocean. *Global Biogeochem. Cycles*, **16**, 9.

McGillicuddy, D. J., Anderson, D. M., Lynch, D. R. and Townsend, D. W. (2005) Mechanisms regulating large-scale seasonal fluctuations in *Alexandrium fundyense* populations in the Gulf of Maine: results from a physical–biological model. *Deep Sea Res. Part II: Top. Stud. Oceanogr.*, **52**, 2698–2714.

Mitarai, S., Siegel, D. A., Watson, J. R., Dong, C. and McWilliams, J. C. (2009) Quantifying connectivity in the coastal ocean with application to the Southern California Bight. *J. Geophys. Res. Oceans*, **114**, C10026.

Moorthi, S. D., Countway, P. D., Stauffer, B. A. and Caron, D. A. (2006) Use of quantitative real-time PCR to investigate the dynamics of the red tide dinoflagellate *Lingulodinium polyedrum*. *Microbial. Ecol.*, **52**, 136–150.

Nezlin, N. P. and Li, B.-L. (2003) Time-series analysis of remote-sensed chlorophyll and environmental factors in the Santa Monica–San Pedro Basin off Southern California. *J. Mar. Syst.*, **39**, 185–202.

Nezlin, N. P., Sutula, M. A., Stumpf, R. P. and Sengupta, A. (2012) Phytoplankton blooms detected by SeaWiFS along the central and southern California coast. *J. Geophys. Res. Oceans*, **117**, C07004.

Omand, M. M., Feddersen, F., Guza, R. T. and Franks, P. J. S. (2012) Episodic vertical nutrient fluxes and nearshore phytoplankton blooms in Southern California. *Limnol. Oceanogr.*, **57**, 1673–1688.

Omand, M. M., Leichter, J. J., Franks, P. J. S., Guza, R. T., Lucas, A. J. and Feddersen, F. (2011) Physical and biological processes underlying the sudden surface appearance of a red tide in the nearshore. *Limnol. Oceanogr.*, **56**, 787–801.

Parsons, M. L., Dortch, Q. and Eugene, T. R. (2002) Sedimentological evidence of an increase in *Pseudo-nitzschia* (Bacillariophyceae) abundance in response to coastal eutrophication. *Limnol. Oceanogr.*, **47**, 551–558.

Parsons, T. R., Maita, Y. and Lalli, C. M. (1984) *A Manual of Chemical and Biological Methods for Seawater Analysis*. Pergamon Press, Oxford.

Pettersson, L. H. and Pozdnyakov, D. (2013) *Monitoring of Harmful Algal Blooms*. Springer, jointly published with Praxis Publishing, UK.

Raine, R., Mcdermott, G., Silke, J., Lyons, K., Nolan, G. and Cusack, C. (2010) A simple short range model for the prediction of harmful algal events in the bays of southwestern Ireland. *J. Mar. Syst.*, **83**, 150–157.

Reifel, K. M., Corcoran, A. A., Cash, C., Shipe, R. and Jones, B. H. (2013) Effects of a surfacing effluent plume on a coastal phytoplankton community. *Contin. Shelf Res.*, **60**, 38–50.

Sandulescu, M., Hernandez-Garcia, E., Lopez, C. and Feudel, U. (2007) Plankton blooms in vortices: the role of biological and hydrodynamics timescales. *Nonlin. Process. Geophys.*, **14**, 1–12.

Schnetzer, A., Jones, B. H., Schaffner, R. A., Cetinic, I., Fitzpatrick, E., Miller, P. E., Seubert, E. L. and Caron, D. A. (2013) Coastal upwelling linked to toxic *Pseudo-nitzschia australis* blooms in Los Angeles coastal waters, 2005–2007. *J. Plankton Res.*, **35**, 1080–1092.

Schnetzer, A., Miller, P. E., Schaffner, R. A., Stauffer, B. A., Jones, B. H., Weisberg, S. B., Digiacomo, P. M., Berelson, W. M. *et al*. (2007) Blooms of *Pseudo-nitzschia* and domoic acid in the San Pedro Channel and Los Angeles harbor areas of the Southern California Bight, 2003–2004. *Harmful Algae*, **6**, 372–387.

Seegers, B. N., Birch, J. M., Marin, R., Scholin, C. A., Caron, D. A., Seubert, E. L., Howard, M. D. A., Robertson, G. L. *et al*. (2015) Subsurface seeding of surface harmful algal blooms observed through the integration of autonomous gliders, moored environmental sample processors, and satellite remote sensing in southern California. *Limnol. Oceanogr.*, **60**, 754–764.

Seubert, E. L., Gellene, A. G., Howard, M. D. A., Connell, P., Ragan, M., Jones, B. H., Runyan, J. and Caron, D. A. (2013) Seasonal and annual dynamics of harmful algae and algal toxins revealed through weekly monitoring at two coastal ocean sites off southern California, USA. *Environ. Sci. Pollut. Res.*, **20**, 6878–6895.

Shipe, R. F., Leinweber, A. and Gruber, N. (2008) Abiotic controls of potentially harmful algal blooms in Santa Monica Bay, California. *Contin. Shelf Res.*, **28**, 2584–2593.

Trainer, V. L., Adams, N. G., Bill, B. D., Stehr, C. M., Wekell, J. C., Moeller, P., Busman, M. and Woodruff, D. (2000) Domoic acid production near California coastal upwelling zones, June 1998. *Limnol. Oceanogr.*, **45**, 1818–1833.

Utermöhl, H. (1958) Zur Vervollkommnung der qualitativen Phytoplanktonmethodik. *Int. Ver. Limnol.*, **9**, 1–38.

Watson, J. R., Mitarai, S., Siegel, D. A., Caselle, J. E., Dong, C. and McWilliams, J. C. (2010) Realized and potential larval connectivity in the Southern California Bight. *Mar. Ecol. Prog. Ser.*, **401**, 31–48.